

Sampling of Glycan-Bound Conformers by the Anti-HIV Lectin *Oscillatoria agardhii* agglutinin in the Absence of Sugar**

Marta G. Carneiro, Leonardus M. I. Koharudin, David Ban, T. Michael Sabo, Pablo Trigo-Mourino, Adam Mazur, Christian Griesinger, Angela M. Gronenborn, and Donghan Lee*

Abstract: Lectins from different sources have been shown to interfere with HIV infection by binding to the sugars of viral-envelope glycoproteins. Three-dimensional atomic structures of a number of HIV-inactivating lectins have been determined, both as free proteins and in glycan-bound forms. However, details on the mechanism of recognition and binding to sugars are elusive. Herein we focus on the anti-HIV lectin OAA from *Oscillatoria agardhii*: We show that in the absence of sugars in solution, both the sugar-free and sugar-bound protein conformations that were observed in the X-ray crystal structures exist as conformational substates. Our results suggest that glycan recognition occurs by conformational selection within the ground state; this model differs from the popular “excited-state” model. Our findings provide further insight into molecular recognition of the major receptor on the HIV virus by OAA. These details can potentially be used for the optimization and/or development of preventive anti-HIV therapeutics.

Oscillatoria agardhii agglutinin (OAA) possesses potent and broad-spectrum activity against the human immunodeficiency virus (HIV). It binds the high-mannose glycans on the viral protein gp120 and thereby interferes with viral entry.^[1–5]

In particular, the OAA carbohydrate-recognition epitope on a high-mannose glycan was identified as 3 α ,6 α -mannopentaose (the branched core unit of Man-9), which is a unique recognition element to OAA-family lectins; it is not recognized by any other anti-HIV lectins.^[2,6,7] The X-ray crystal structures of both free and glycan-bound OAA revealed a β -barrel-like structure with two symmetrically positioned glycan binding sites at opposite ends of the barrel.^[3] In the presence of sugar, the protein structure in binding site 2 shows a conformational change, namely, the orientation of the peptide bond between W77 and G78 is flipped by approximately 180°. The equivalent peptide bond in binding site 1 (W10–G11), in contrast, is essentially identical in the absence and in the presence of sugar; that is, it adopts the bound conformation even without any glycan present, possibly owing to protein–protein contacts within the crystal.^[3] To elucidate the general mechanism underlying glycan recognition by OAA, we investigated the conformational properties sampled by the protein in solution by NMR spectroscopy.

Carr–Purcell–Meiboom–Gill (CPMG) relaxation dispersion experiments^[8,9] have become popular tools for studying conformational exchange on the microsecond-to-millisecond time scale. They provide thermodynamic (relative populations), kinetic (rates of exchange), and structural information (chemical shift differences) on sparsely populated and transient conformers,^[10] termed excited states, that are structurally different from the most populated state, termed ground state. To investigate whether the conformers associated with sugar binding are already sampled in solution in the absence of sugar, we measured ¹⁵N CPMG relaxation dispersion on sugar-free OAA. At 298 K, we found that 22 residues undergo conformational exchange. However, at this temperature, the conformational exchange is fast on the chemical shift time scale, and therefore chemical shift differences between the ground and excited states could not be extracted. When the temperature was lowered to 277 K, amide resonances of 60 amino acids underwent conformational exchange (Figure 1 A,B), with the affected amino acids spread throughout the entire protein and not restricted to the binding sites (as highlighted by the blue spheres in Figure 1 A). In contrast, residues associated with significant amide ¹⁵N chemical shift changes upon interaction with α 3, α 6-mannopentaose are confined to the binding sites (Figure 1 C). More importantly, for 22 amides, exchange is slow on the chemical shift time scale at this temperature (see the Supporting Information), and structural information about the exchanging or “excited” state can be extracted in the form of chemical shift differences ($\Delta\omega$) obtained from the analysis of the dispersion profiles (see Table S1 in the Supporting

[*] M. G. Carneiro, D. Ban,^[†] T. M. Sabo, P. Trigo-Mourino, A. Mazur,^[††] C. Griesinger, D. Lee

Department for NMR-Based Structural Biology
Max Planck Institute for Biophysical Chemistry
Am Fassberg 11, 37077 Göttingen (Germany)
E-mail: dole@nmr.mpiibpc.mpg.de

L. M. I. Koharudin, A. M. Gronenborn
Department of Structural Biology
University of Pittsburgh School of Medicine
1050 Biomedical Science Tower 3, 3501 5th Avenue
Pittsburgh, PA 15260 (USA)

[†] Present address: St. Jude Children’s Research Hospital
Department of Structural Biology
262 Danny Thomas Place, Memphis, TN 38105 (USA)

[††] Present address: Biozentrum, University of Basel
Klingelbergstrasse 70, 4056 Basel (Switzerland)

[**] This research was supported by the Humboldt Foundation (post-doctoral fellowship to P.T.M.), National Institutes of Health grant GM080642 (to A.M.G.), the Max Planck Society, and the EU (ERC grant agreement number 233227 to C.G.). The solution NMR structure of free OAA has been deposited in the Protein Data Bank (accession code: 2MWH). The NMR spectroscopic data used for structural calculation have been deposited in the Biological Magnetic Resonance Data Bank (accession code: 25324). HIV = human immunodeficiency virus.



Supporting information for this article is available on the WWW under <http://dx.doi.org/10.1002/anie.201500213>.

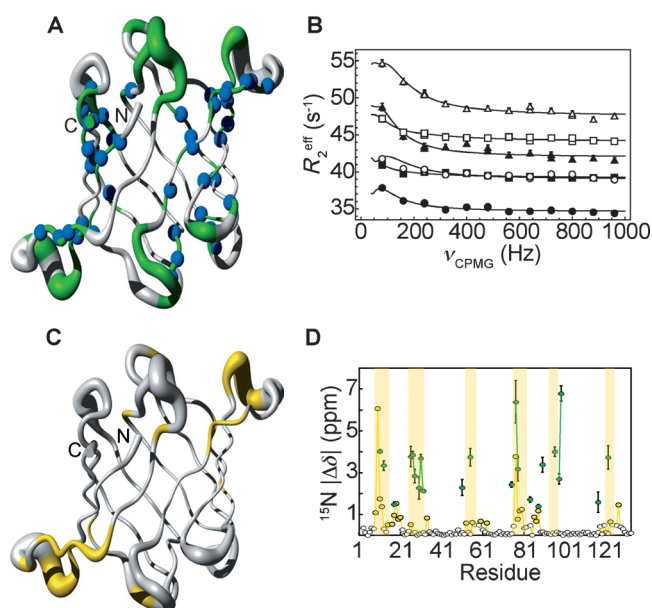


Figure 1. Sugar-free OAA samples a high-energy state that does not resemble the sugar-bound state. A) Residues that undergo conformational exchange on the microsecond-to-millisecond time scale are colored green. Blue spheres indicate residues outside of the sugar-binding sites. B) ^{15}N relaxation dispersion curves of M51 (triangles), W90 (circles), and T117 (squares) amide resonances. Solid lines are the best fits to a two-state exchange model on a per-residue basis. All relaxation dispersion data were recorded at two fields (800 MHz, empty symbols; 600 MHz, full symbols). Experimental errors were estimated on the basis of duplicate measurements and are within the size of each symbol. C) Residues whose amide resonances are significantly perturbed upon the addition of sugar (yellow) are in general confined to the binding sites. D) The ^{15}N chemical shift differences ($|\Delta\delta|$) between the ground and the excited state sampled by sugar-free OAA as extracted from the CPMG experiment (green circles) are different from those measured directly from spectra of the sugar-free and sugar-bound OAA protein (yellow circles). The white circles represent residues that do not exhibit any significant chemical shift perturbation upon the addition of sugar. Areas associated with sugar binding are shaded yellow.

Information). These values can be directly compared with the chemical shift differences extracted from ^1H - ^{15}N HSQC spectra of sugar-free and sugar-saturated OAA samples. If they were identical, the excited state sampled by the sugar-free protein would correspond to the sugar-bound state. However, in the case of OAA, the chemical shift differences between the ground and excited states, as derived from CPMG relaxation dispersion, differ from those measured in the

sugar-free and sugar-bound ^1H - ^{15}N HSQC spectra (Figure 1D; see also Figure S1 in the Supporting Information). Both the diverse spatial distribution of residues associated with CPMG relaxation dispersion and of resonances undergoing chemical shift changes upon the addition of $\alpha,3,\alpha$ -mannopentaose, as well as their non-correlation, suggest that the excited state that is sampled by the sugar-free protein in solution does not correspond to the sugar-bound conformation, and may indicate a transient state not related to binding. Notably, the excited state also does not correspond to the unfolded state (see Figure S2).

Conformational fluctuations in solution, potentially relevant for molecular recognition, can occur not only between a ground and an excited state but also within the ground state itself^[11] (i.e., on a time scale faster than that probed by CPMG relaxation dispersion). To explore this possibility, we first determined the solution structure of free OAA. The NMR ensemble of free OAA was determined on the basis of complete assignment^[12] and a large number of experimental constraints (summarized in Table S2) amounting to an average of about 19 constraints per residue. The structure is well-defined as judged by atomic root-mean-square deviation (RMSD) values relative to the mean coordinates of (0.7 ± 0.1) and (0.33 ± 0.05) Å for all backbone atoms and those in secondary structure elements, respectively. No violations of experimental constraints are present in the final ensemble. The solution structure of OAA exhibits a β -barrel fold made up of 10 antiparallel β -strands comprising residues 3–9, 18–24, 33–40, 46–53, 58–65, 70–76, 84–91, 100–106, 113–120, and 126–132 (Figure 2A). It closely resembles the sugar-free and sugar-bound X-ray crystal structures, as evidenced by backbone RMSD values of 0.7 and 0.67 Å, respectively. The two previously identified carbohydrate-binding sites,^[2,3] encompassing the loops between β 1– β 2, β 7– β 8, and β 9– β 10 (site 1) and β 2– β 3, β 4– β 5, and β 6– β 7 (site 2), are highlighted in Figure 2B,C, respectively.

Previously, we noted that the sugar-free and sugar-bound X-ray crystal structures exhibited different peptide-bond conformations for W77 and G78 in binding site 2, as typified

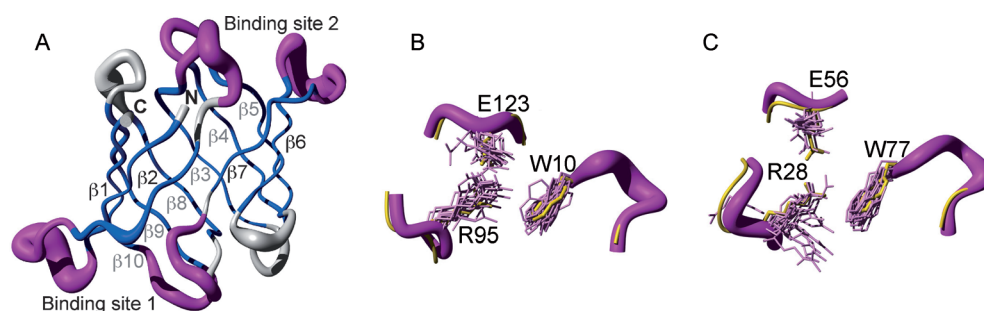


Figure 2. The solution structure of the anti-HIV protein OAA samples the bound conformation. A) The overall fold of the sugar-free solution structure of OAA comprises 10 antiparallel β -strands (blue) that form a β -barrel very similar to the sugar-free and sugar-bound X-ray crystal structures (PDB code: 3S5V and 3S5X,^[3] respectively). B) Details of the conformation of binding site 1. C) Details of the conformation of binding site 2. The two sugar-binding sites (magenta) resemble the sugar-bound conformation of the X-ray crystal structure (yellow). Side chains directly involved in carbohydrate binding (W10, R95, and E123 in site 1 and R28, E56, and W77 in site 2) are shown in stick representation. The mean positions of the backbone C^α atoms are shown in tube representation, with the radius of the tube corresponding to the average deviation of all conformers with respect to the mean.

by characteristic distances between the backbone amide protons (H^N) of these two residues: the very short distance (2.2 Å) in the absence of sugar is increased to 4.4 Å in the bound conformation (Figure 3A). Given the steep distance

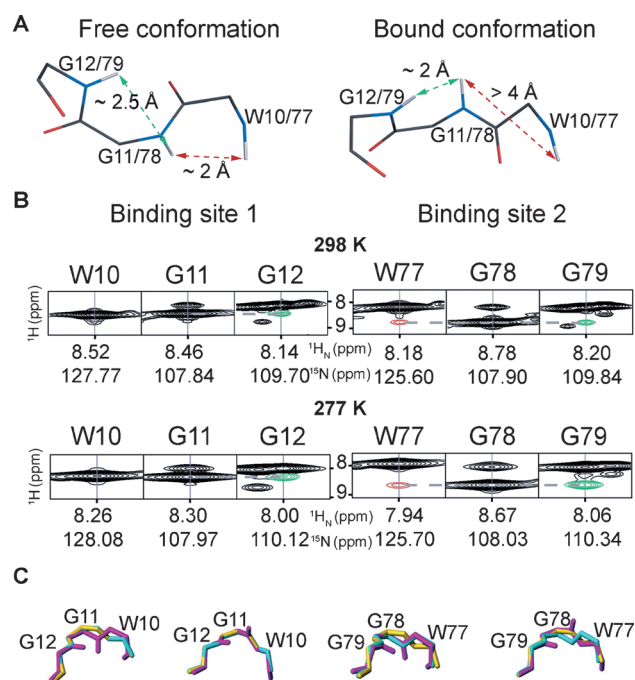


Figure 3. Backbone amide distances measured in solution by NMR spectroscopy are sensitive measures of a flipped peptide bond.

A) Stick representations of the backbone conformations in the sugar-free and sugar-bound crystal structures (PDB code: 3S5V and 3S5X,^[3] respectively). The distance between the backbone amide hydrogen atoms (H^N) of W77 and G78 in site 2 (dashed red arrows) is short (2.2 Å) in the sugar-free conformation and longer (4.4 Å) in the sugar-bound conformation. Binding site 1 displays the sugar-bound conformation in the sugar-free crystal structure owing to protein–protein contacts within the crystal. B) NOE cross-peaks corresponding to the distances depicted in (A) between H^N W77 and H^N G78 (red) and between H^N G11/G78 and H^N G12/G79 (green) at different temperatures (298 K, top; 277 K, bottom). The intensity ratio between these NOE cross-peaks indicates that both the sugar-free and sugar-bound conformations are present. C) The different backbone conformations sampled by OAA in solution (magenta) match the sugar-free (cyan) and sugar-bound conformations (yellow) seen in both binding sites in the X-ray crystal structures.

(d) dependence ($1/d^6$) of the nuclear Overhauser effect (NOE), such a distinct difference in distance is uniquely suited to be analyzed by NOE measurements. Indeed, in the NOESY spectrum of OAA saturated with glycan, a very weak cross-peak at the noise level was observed between H^N W77 and H^N G78 (see Figure S3), which is consistent with an interatomic distance larger than 4 Å. In contrast, in the absence of sugar, a sizable NOE cross-peak between H^N W77 and H^N G78 was present (Figure 3B). However, the intensity of the latter was much smaller than expected from the distance in the X-ray crystal structure, as compared to the NOE cross-peak between H^N G78 and H^N G79. The experimental peak intensities can be reconciled with the

structural data if both the free and the bound conformation are present at 298 K with relative populations of about 10% of the sugar-free and 90% of the sugar-bound conformation observed in the crystal (see Table S3; details of the estimation of relative populations on the basis of NOE spectroscopic data are provided in the Supporting Information). At 277 K, a precise quantitative analysis is prohibited owing to spectral overlap; however, a qualitative evaluation of the NOESY spectrum (Figure 3B) suggests that the equilibrium is likewise skewed towards the sugar-bound conformation observed by X-ray crystallography. Interestingly, individual conformers of the solution structure ensemble exhibit backbone conformations resembling the sugar-free and sugar-bound X-ray crystal structures in both binding sites (Figure 3C).

Whereas NOE values report on distances, three-bond J coupling constants (3J) provide complementary structural data owing to their dependence on dihedral angles.^[13] Of special interest in this case are $^3J(H^N, H^\alpha)$ coupling constants, which depend on the φ dihedral angle and are therefore exquisitely sensitive to peptide-bond flips. For glycine residues, which contain two H^α hydrogen atoms, two different $^3J(H^N, H^\alpha)$ coupling constants can be measured if non-degenerate H^α resonances exist. These coupling constants depend on the angle θ :^[13]

$$^3J(H^N, H^\alpha) = A \cos^2 \theta + B \cos \theta + C$$

with $\theta = \varphi - 60^\circ$ for $H^{\alpha 3}$ (pro-*S*) and $\theta = \varphi + 60^\circ$ for $H^{\alpha 2}$ (pro-*R*), and $A = (7.13 \pm 0.34)$, $B = -(1.31 \pm 0.13)$, and $C = (1.56 \pm 0.34)$ Hz.^[14] We stereospecifically assigned the H^α glycine resonances of G11 and G78 by comparing both H^N – H^α NOE cross-peak intensities with the interatomic distances derived from the X-ray crystal structures (see Figure S4). As for the H^N – H^N distances described above, the NOE intensities from sugar-bound OAA are in good agreement with the sugar-complexed X-ray crystal structure, whereas the NOE intensities in sugar-free OAA are better explained if a mixture of approximately 10% of the free and 90% of the bound conformation is assumed (see Table S3).

For an accurate analysis of 3J coupling constants between geminal hydrogen atoms, an estimation of the flip rates for the peptide bond is required.^[15] Nonetheless, even without this rate, the H^N – H^α coupling constants associated with each φ angle can be evaluated qualitatively (see Figure S5 and Table S4). Again, the $^3J(H^N, H^\alpha)$ coupling constants of sugar-bound OAA are in good agreement with those predicted on the basis of the sugar-complexed X-ray crystal structure (i.e., the larger $^3J(H^N, H^\alpha)$ coupling is associated with $H^{\alpha 2}$, and the smaller $^3J(H^N, H^\alpha)$ coupling is associated with $H^{\alpha 3}$). In contrast, the experimental $^3J(H^N, H^\alpha)$ coupling constants of G11 and G78 for sugar-free OAA are of opposite size to those predicted from the free X-ray crystal structure, thus suggesting that the conformational equilibrium is skewed towards the sugar-bound conformation observed in the crystal (see Table S4).

Our present results show that not only is the sugar-bound conformation sampled in the absence of sugar but that it is thermodynamically more favorable (larger population) than the sugar-free conformation. Furthermore, the X-ray crystal-

lographic data of sugar-free OAA suggests structural flexibility in binding site 2 (see Figure S6), and the inspection of additional X-ray crystal structures that are available for several OAA homologues, with high conservation of binding-site residues and sugar–protein interactions,^[6,7] revealed that the sugar-bound conformation is frequently seen in sugar-free structures, thus reinforcing the notion that the bound conformation is more favorable in solution. This hypothesis agrees with the observation that the motion detected by CPMG relaxation dispersion experiments between the ground and excited state—motion that occurs on a slower time scale than that observed in the NOE experiments—does not coincide with the chemical shift differences in the ¹H–¹⁵N HSQC spectra of glycan-free and -bound OAA. Therefore, these structural changes are probably associated with motions within the ground state.

Altogether, our findings show that in solution the sugar-free (10%) and the sugar-bound (90%) protein conformations coexist in equilibrium, and that the recognition of 3 α ,6 α -mannopentaose by OAA, which determines its anti-HIV activity, could proceed by conformational selection from a ground-state ensemble, since the bound conformation is abundantly present. These results provide detailed insight into the molecular recognition mechanism associated with the anti-HIV activity of OAA. A thorough understanding of this mechanism may guide the further development of this lectin as a potent microbicide: the fact that the sugar-bound conformation is highly populated in the absence of sugar suggests that only minimal changes in conformational entropy upon binding are at play in terms of the protein backbone. However, backbone conformational fluctuations could affect the conformational entropy of the side chains through a hierarchy of motions by a population-shuffling mechanism.^[16] Efforts to optimize the affinity of OAA for 3 α ,6 α -mannopentaose should therefore primarily be focused on enhancing the enthalpic contribution to the binding energetics, without disregarding entropic effects.

Keywords: anti-HIV lectins · conformational selection · ground state · NMR spectroscopy · proteins

How to cite: *Angew. Chem. Int. Ed.* **2015**, *54*, 6462–6465
Angew. Chem. **2015**, *127*, 6562–6565

- [1] Y. Sato, S. Okuyama, K. Hori, *J. Biol. Chem.* **2007**, *282*, 11021–11029.
- [2] L. M. I. Koharudin, W. Furrey, A. M. Gronenborn, *J. Biol. Chem.* **2011**, *286*, 1588–1597.
- [3] L. M. I. Koharudin, A. M. Gronenborn, *Structure* **2011**, *19*, 1170–1181.
- [4] D. Huskens, D. Schols, *Mar. Drugs* **2012**, *10*, 1476–1497.
- [5] G. Férir, D. Huskens, S. Noppen, L. M. I. Koharudin, A. M. Gronenborn, D. Schols, *J. Antimicrob. Chemother.* **2014**, *69*, 2746–2758.
- [6] L. M. I. Koharudin, S. Kollipara, C. Aiken, A. M. Gronenborn, *J. Biol. Chem.* **2012**, *287*, 33796–33811.
- [7] M. J. Whitley, W. Furey, S. Kollipara, A. M. Gronenborn, *FEBS J.* **2013**, *280*, 2056–2067.
- [8] H. Y. Carr, E. M. Purcell, *Phys. Rev.* **1954**, *94*, 630–638.
- [9] S. Meiboom, D. Gill, *Rev. Sci. Instrum.* **1958**, *29*, 688–691.
- [10] A. G. Palmer, C. D. Kroenke, J. P. Loria, *Methods Enzymol.* **2001**, *339*, 204–239.
- [11] O. F. Lange, N.-A. Lakomek, C. Farès, G. F. Schröder, K. F. A. Walter, S. Becker, J. Meiler, H. Grubmüller, C. Griesinger, B. L. de Groot, *Science* **2008**, *320*, 1471–1475.
- [12] M. G. Carneiro, L. M. Koharudin, C. Griesinger, A. M. Gronenborn, D. Lee, *Biomol. NMR Assignments* **2015**, in press.
- [13] M. Karplus, *J. Am. Chem. Soc.* **1963**, *85*, 2870–2871.
- [14] M. Habeck, W. Rieping, M. Nilges, *J. Magn. Reson.* **2005**, *177*, 160–165.
- [15] G. W. Vuister, A. Bax, *J. Am. Chem. Soc.* **1993**, *115*, 7772–7777.
- [16] C. A. Smith, D. Ban, S. Pratihari, K. Giller, C. Schwiegk, B. L. de Groot, S. Becker, C. Griesinger, D. Lee, *Angew. Chem. Int. Ed.* **2015**, *54*, 207–210; *Angew. Chem.* **2015**, *127*, 209–212.

Received: January 9, 2015

Revised: March 16, 2015

Published online: April 14, 2015